Author/s:
Gu, H;Yan, L;Saxena, S;Shi, X;Zhang, X;Li, Z;Luo, Q;Zhou, H;Yang, Y;Liu, X;Wong, WWH;Ma, C-Q

Title:
Revealing the Interfacial Photoreduction of MoO3 with P3HT from the Molecular Weight-Dependent "Burn-In" Degradation of P3HT:PC61BM Solar Cells

Date:
2020-10-26

Citation:
Gu, H., Yan, L., Saxena, S., Shi, X., Zhang, X., Li, Z., Luo, Q., Zhou, H., Yang, Y., Liu, X., Wong, W. W. H. & Ma, C. -Q. (2020). Revealing the Interfacial Photoreduction of MoO3 with P3HT from the Molecular Weight-Dependent "Burn-In" Degradation of P3HT:PC61BM Solar Cells. ACS Applied Energy Materials, 3 (10), pp.9714-9723. https://doi.org/10.1021/acsaem.0c01325.

Persistent Link:
https://hdl.handle.net/11343/344897

Revealing the Interfacial Photoreduction of MoO_3 with P3HT From the Molecular Weight-Dependent "Burn-in" Degradation of P3HT:$PC_{61}BM$ Solar Cells

Huimin Gu,[a,b] Lingpeng Yan,[b,c] Sonam Saxena,[d] Xuning Zhang,[e,f] Zerui Li,[b] Qun Luo,[b] Huiqiong Zhou,[e] Yongzhen Yang,[a,*] Xuguang Liu,[a,c] Wallace W. H. Wong,[d] Chang-Qi Ma,[b,*]

[a] Key Laboratory of Interface Science and Engineering in Advanced Materials, Ministry of Education, Taiyuan University of Technology, Taiyuan 030024, P. R. China

[b] Printable Electronics Research Center, Suzhou Institute of Nano-Tech and Nano-Bionic, Chinese Academy of Sciences (CAS), Suzhou 215123, P. R. China

[c] Institute of New Carbon Materials, Taiyuan University of Technology, 79 Yingze Street, Taiyuan 030024, P. R. China.

[d] ARC Centre of Excellence in Exciton Science, School of Chemistry, Bio21 Institute, University of Melbourne, Parkville, Victoria 3010, Australia

[e] CAS Key Laboratory of Nanosystem and Hierarchical Fabrication, CAS Center for Excellence in Nanoscience, National Center for Nanoscience and Technology, Beijing 100190, China

[f] School of Chemistry, Beijing Advanced Innovation Center for Biomedical Engineering, Beihang University, Beijing 100191, P. R. China

*Corresponding Author: yyztyut@126.com; cqma2011@sinano.ac.cn

Abstract:

"Burn-in" degradation occurs in many polymer solar cell systems, which reduces the overall power output of the cells. Understanding "burn-in" degradation mechanism is therefore highly important to improving device stability. In this manuscript, the decay behaviors of P3HT:$PC_{61}BM$ solar cells depending on the molecular weight of P3HT were systematically investigated. Although all these P3HTs were highly crystalline with regioregularity of 94%97%, the stability of P3HT:$PC_{61}BM$ cells showed a nonmonotonic dependence on P3HT molecular weight. The cells based on P3HT with a weight average molecular weight (M_w) of 20 K showed much faster decadence in open circuit voltage (V_{OC}) and fill factor (FF) during aging, yielding a lowest performance stability in comparison with the cells based on P3HT of 10 K, 25 K, and 30 K. UV-Vis absorption and external quantum efficiency (EQE) spectra demonstrated that the performance decay should not be attributed to the change in photoactive layer. The recovery of V_{OC} and FF of the aged cells after renewing MoO_3/Al electrode revealed that degradation of MoO_3/Al is the main reason for the V_{OC} and FF decays. Increased absorption over 400-650 nm was measured for the model MoO_3/P3HT film under light illumination. Meanwhile, X-ray photoelectronic spectroscopy (XPS) confirmed that Mo (VI) was partially reduced under light illumination. These results demonstrate that photon chemical reduction (PCR) of MoO_3 by P3HT occurred during aging, which is then thus ascribed as the essential reason for the fast V_{OC} and FF decays of the cells. The surface morphology of the photoactive layer measured by atomic force microscope (AFM) revealed the much rougher surface of P3HT-20 K:$PC_{61}BM$ film . Such a rough surface increases the contact area between P3HT and MoO_3, and consequently enhances the PCR of MoO_3 and P3HT, which is considered as the main reason for the molecular weight-dependent degradation behaviors. For the first time, the current work clearly demonstrates that photoreduction of metal oxide and photoactive layer would lead to fast V_{OC} and FF decays, which could be a very important degradation pathway for polymer solar cells

Key Words

polymer solar cells; stability; "burn-in" degradation; interface decay; photon chemical reduction; surface morphology

Introduction

Conjugated polymer based solar cells, named also bulk-heterojunction solar cells, have many advantages of flexibility, lightweight, excellent compatibility with low-temperature printing processing, and have attracted much attention in the last few years.[1-3] High power conversion efficiencies (PCE) of more than 16%[4-6] and 17%[7] were reported for the single and tandem junction cells, demonstrating excellent application prospects for the next future. Although there are a few papers reporting the stable polymer solar cells with operation lifetime of 7-10 years,[8-10] Statistical data revealed that the stability of polymer solar cells is far from satisfaction.[11] Understanding the degradation mechanism and improving the operation lifetime of polymer solar cells have become the next key challenge for polymer solar cells before commercialization.

It is known that most of polymer:fullerene solar cells suffer a fast "burn-in" degradation, which dramatically reduces the overall power output of the cells.[12-13] Recent works demonstrated that the dimerization of $PC_{61}BM$ is one of the main reasons for the "burn-in" degradation of polymer:fullerene solar cells,[14-16] while the morphology of photoactive layer plays an important role in influencing the "burn-in" degradation process. For example, Brabec *et al.* demonstrated that for crystalline polymers, relatively pure donor and acceptor domains formed within photoactive layer, which reduces the charge recombination and makes this type of cells insensitive to energetic disorder. Therefore, open-circuit voltage (V_{OC}) of these cells is rather stable during aging. However, the formation of pure electron acceptor domain promotes the photon-induced dimerization of fullerene molecules, therefore fast short circuit current (J_{SC}) decay is usually found for this type of cell.[15] In contrast, for amorphous polymers, donor and acceptor molecules are well intermixed in the blend film, which makes this type of cell sensitive to energetic disorder but insensitive to the photon dimerization of fullerenes. Therefore, fast V_{OC} decays and rather stable J_{SC} are typically found for this type of cell.[17-18] Our recent work also demonstrated that the fast J_{SC} decay of polymer:fullerene solar cells is directly correlated to the external load attached to the

cells during aging, that is, to the concentration of high energy excitons within the blend film.[16] In addition to the photodimerization of $PC_{61}BM$, very recently, Brabec *et al.* demonstrated that spinodal donor-acceptor demixing also led to fast J_{SC} decay in polymer:fullerene solar cells,[19] which is considered as the third fast degradation pathway to the polymer:fullerene solar cells.

Besides the change in photoactive layer, variation of interface property also influences device performance as well. For example, McGehee *et al*. found that the molecular thermal motion of polymers and fullerenes at the operating temperature increased their adhesion to interfacial layer, which in turn created a barrier layer for charge extraction that degrades device performance.[20] Zhou *et al.* demonstrated that the UV light induced decomposition of nonfullerene acceptor by ZnO led to poor device performance,[21] which could be improved by using UV-light inert SnO_2. Later Park and Son reported also the intrinsic photo-degradation of polymer solar cells caused by UV-light induced decomposition of the non-fullerene acceptor component.[22]

From the molecular structure point of view, regioregularity[23-24] and molecular weight[25-26] are key parameters defining conjugated polymers for the application in solar cells. Both factors can influence performance and stability of polymer solar cells. Although the influence of the molecular weight on photovoltaic performance has been reported,[27-29] there is no paper discussing the influence of molecular weight on device stability. Understanding this will help understand the specific degradation behaviors of polymer solar cells, and will guide the optimization of polymers for use in polymer solar cells.

In this work, we systematically investigated the influence of the molecular weight of P3HT on the "burn-in" degradation behavior of P3HT:$PC_{61}BM$ solar cells. Results indicated that the stability of P3HT:$PC_{61}BM$ cells was not monotonously dependent on the molecular weight of P3HT. P3HT - 20 K showed the lowest device stability, while the polymers with higher or lower molecular weight (10 K, 25 K, 30 K) showed better device stability. For P3HT-20 K based cells, V_{OC} and fill factor (FF) decays dominate the overall performance loss. Spectroscopic studies confirmed that the photon-chemical reduction (PCR) of MoO_3 by P3HT occurred during aging, which was believed to be

the main reason for the fast V_{OC} and FF "burn-in" decays. Surface morphology analyses revealed that the rougher surface of P3HT-20K:$PC_{61}BM$ films which increased the interaction between P3HT and MoO_3, and then induced the poorer device stability of the P3HT-20K based cells. These results demonstrate that interface photon-chemical reaction has a significant influence on the stability of polymer solar cells, and a smoother surface could help achieve higher device stability.

Experiment Part:

1. Materials

Regioregular poly(3-hexylthiophene-2,5-diyl)s (P3HT-10 K, $M_w = 1.16\times10^4$ g/mol, Đ (Dispersity) = 1.15, regioregularity Rr = 94.3%; P3HT-20 K, $M_w = 2.12\times10^4$ g/mol, Đ = 1.11, regioregularity Rr = 96.1%; P3HT-25 K, $M_w = 2.64\times10^4$ g/mol, Đ = 1.40, regioregularity Rr = 97.1%; P3HT-30 K, $M_w = 3.05\times10^4$ g/mol, Đ = 1.37, regioregularity Rr = 97.1%;) were synthesized by a Ni-catalyzed metathesis coupling reaction accordingly to the literature.[30] [6,6]-Phenyl-C_{61}-butyric acid methyl ester ($PC_{61}BM$) was purchased from Solenne B.V.. Molybdenum oxide (MoO_3) was purchased from Strem Chemicals, Inc., America. Sodium hydroxide (NaOH) was purchased from Sinopharm Chemical Reagent Co. LTD., China. All materials were used as received. Zinc oxide nanoparticles (ZnO) were prepared through the reaction of KOH and $Zn(OAc)_2$ in methanol solvent as reported by Beek et al.[31]

2. Method for solar cell fabrication

The devices were fabricated from patterned ITO glass (Shenzhen Southern China City Hunan Technology Co. Ltd.). The substrates were sequentially sonically cleaned in detergent, deionized water, acetone, and isopropanol, and finally treated in UV-ozone oven for 30 min. First, filtered ZnO (12 mg/mL in methanol) was spin-coated on ITO substrates at 2000 rpm for 60 s. Then, the samples were annealed at 130 ºC for 10 min on a hot plate. A blend solution of P3HT and $PC_{61}BM$ in ortho-dichlorobenzene (ODCB) (1:1(w/w), 40 mg /mL) was spin-coated on the top of ZnO layer at 600 rpm for 60 s. The wet P3HT:$PC_{61}BM$ blend films were then put into covered Petri dishes for 1.5

hours.[16] The samples were subsequently heated at 125 ºC for 10 min. Finally, MoO_3 (10 nm) and Al (100 nm) were sequentially vacuum deposited on the top of the active layer as hole-extraction layer and anode, respectively. The size of the substrate was 2.5 cm×2.5 cm, and the effective photovoltaic area, defined by the geometrical overlap between the bottom cathode electrode and the top anode, was 0.09 cm^2. As for the renewal of MoO_3/Al, the electrode of fresh or aged cells was removed by sodium hydroxide solution (0.2 mg/mL). After that, MoO_3 (10 nm) and Al (100 nm) were sequentially vacuum deposited again according to the standard protocol.

3. Thin film preparation and characterization

The model thin films for light illumination test were prepared by spin-coating corresponding solution to cleaned ITO substrates. UV-Vis absorption spectrum was measured by a Lambda 750 UV/ Vis /NIR spectrophotometer (PerkinElmer). X-ray photoelectron spectroscopy (XPS) measurements were performed ona PHI 5000 Versa Probe III. The XPS sample was prepared on a glass substrate of 1 cm×1 cm that fully cover ITO. Atomic force microscope (AFM) images of the films were measured with the Park XE-120 microscope using Cr/Au-coated conducting tips (NSC18, Mikromasch, Tallinn, Estonia). Transmission electron microscopy (TEM) images of active layers were obtained using a Tecnai G2 F20 S-Twin 200 kV field-emission electron microscope (FEI). The photoactive layers for TEM measurement were prepared by spin-coating the solution onto cleaned glass substrate, followed by a treatment of HF vapor in fume hood.

4. Photovoltaic performance and stability characterizations

PCE of devices was measured in a N_2-filled glove box using a Keithley 2400 source meter under illumination with simulated AM 1.5G sunlight (Verasol-2, LED 3A Sun simulator, Newport). EQE spectra were recorded under illumination by a simulated one sun operation condition using bias light from a 532 nm solid state laser. Light from a 150 W tungsten halogen lamp (Osram 64610) was used as a probe light and was modulated with a mechanical chopper before passing through the monochromator

(Zolix, Omni-k300) to select the wavelength. The response was recorded as the voltage by an I–V converter (DNR-IV Convertor, Suzhou D&R Instruments), using a lock-in amplifier (Stanford Research Systems SR 830). A calibrated Si cell was used as a reference. The device for EQE measurement was kept behind a quartz window in a nitrogen-filled container. The long-term stability of un-encapsulated devices was conducted using a multi-channel solar cell performance decay test system (PVLT-G8001M, Suzhou D&R Instruments Co. Ltd.) under a testing condition in accordance with ISOS-L-1. The devices were put inside a glove box (H_2O < 1 ppm, O_2 < 1 ppm), and continuously illuminated with white LED light (D&R Light, L-W5300KA-150, Suzhou D&R Instruments). The illumination light intensity was initially set so the output J_{SC} equaled the J_{SC} measured under standard conditions. The illumination light intensity was monitored by a photodiode (Hamamtsu S1336-8BQ). current-voltage (*J–V*) curves of the devices were checked periodically, and the photovoltaic performance data (V_{OC}, J_{SC}, FF, and PCE) were calculated automatically accordingly to the *J–V* results. Highly sensitive EQE curves spectra were measured by a Solar Cell Spectral Response Measurement System PECT-600 (Enlitech, Taiwan，China).

Results and Discussions

1. Molecular weight depended device performance of P3HT:$PC_{61}BM$ cells

Regioregular P3HTs with different molecular weights were synthesized by a Ni-catalyzed metathesis coupling reaction.[30] Molecular weight of the polymer was controlled by tuning the feeding ratio of catalyst to monomer. Four different P3HTs with weight average molecular weight (Mw) of 1.16×10^4 g/mol (denoted as P3HT-10 K), 2.12×10^4 g/mol (P3HT-20 K), 2.64×10^4 g/mol (P3HT-25 K), 3.05×10^4 g/mol (P3HT-30 K) were chosen as the polymers for investiation molecular weight dependent degradation behaviors. It is worth noting that all these polymers have high regioregularity of 94%-97%, which is an important parameter for P3HT materials. **Figure 1** shows the *J-V* curves and EQE spectra of the P3HT:$PC_{61}BM$ cells and **Table 1** lists the photovoltaic performance data. Statistical photovoltaic data are shown in

Figure S1 in supporting information. All these P3HT:$PC_{61}BM$ solar cells show appropriate power conversion efficiency of 3.5%-3.9%, which is comparable to those reported in the literature.[32] V_{OC} of these cells are around 0.51-0.55 V, which are lower than the common value reported in the literature.[33] This could be attributed to the relatively high regioregularity of the synthesized P3HT.[24] J_{SC} of the cells is found to increase with the increase of molecular weight, which can be attributed to the more optimal nanomorphology of the blend film (*vide infra*).[25, 34] The photovoltaic performance results shown here indicate that the cells are acceptable for stability comparison after careful optimization.

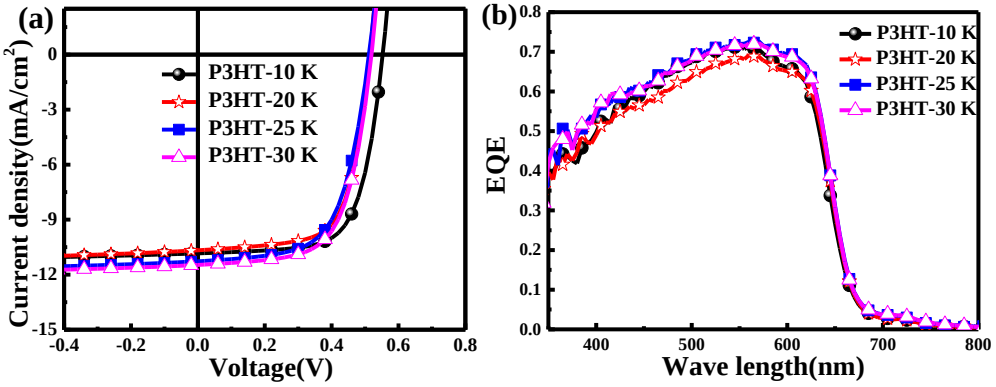

Figure 1. *J-V* curves (a) and EQE spectra (b) of P3HT:$PC_{61}BM$ cells prepared from P3HT with different polymer molecular weights (10 K, 20 K, 25 K and 30 K)

Table 1. Photovoltaic performance data of P3HT:$PC_{61}BM$ cells prepared from P3HT with different molecular weights (10 K, 20 K, 25 K and 30 K)

Sample	Mw (kg/mol)	M_n (kg/mol)	PDI	Rr (%)	V_{OC} (V)	J_{SC} (mA·cm^2)	FF	PCE (%)	T_{80} (h)[a]	PCE^{400} (%)[b]
P3HT-10 K	11.6	10.1	1.15	94.3	0.55±0.01	10.78±0.10	0.67±0.01	3.97±0.10	22.53	38
P3HT-20 K	21.2	19.1	1.11	96.1	0.51±0.01	10.56±0.11	0.66±0.01	3.63±0.10	7.85	10
P3HT-25 K	26.4	18.8	1.40	97.1	0.51±0.00	11.08±0.02	0.62±0.03	3.55±0.07	15.73	43
P3HT-30 K	30.5	22.3	1.37	97.1	0.52±0.01	11.27±0.20	0.64±0.01	3.75±0.05	44.55	67

a: Time that reaches 80% of its initial PCE;

b: the ratio of the PCE aged for 400 hours to its initial value (in percentage)

2. Degradation behaviors of the P3HT:$PC_{61}BM$ cells

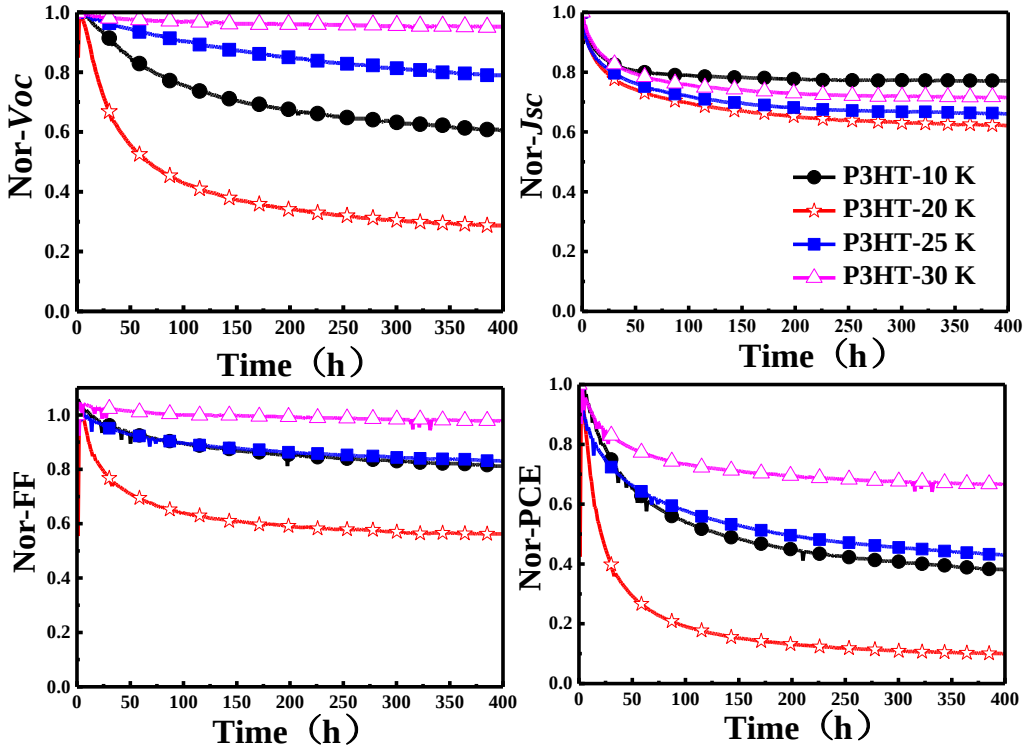

Figure 2. Evolution of V_{OC}, J_{SC}, FF and PCE of the P3HT:$PC_{61}BM$ cells aged under light illumination

Figure 2 depicts the evolution of V_{OC}, J_{SC}, FF, and PCE of the P3HT:$PC_{61}BM$ cells aged at simulated operation condition. **Figure S2** in supporting information showes the changes of *J-V* curves over 400 hours. As seen here, all these cells shows fast "burn-in" degradation, and T_{80}, the time the solar cell reaches 80% of initial device performance, is measured to be 22.53, 7.85, 15.73, and 44.55 h for 10 K, 20K, 25 K, 30 K P3HT cells, respectively (**Table 1**). It is worth noting that all these cells show similar J_{SC} decay rates, independent of the molecular weight of P3HT. Such a fast J_{SC} decay can be attributed to the photon-induced dimerization of $PC_{61}BM$ during aging.[15-16, 35] V_{OC} and FF, on the other hand, show a non-monotonous dependence on the molecular weight of P3HT. The cell based on P3HT-20 K shows the fastest V_{OC} and FF decays, leading to the lowest device performance after aging. PCE after aging for 400 h (PCE^{400}) is only 10% of its initial value, which is much lower than that of the cells based on 10 K, 25 K and 30 K P3HT (38%, 43% and 67%).

Thermal annealing was performed on these aged P3HT:$PC_{61}BM$ cells to check whether such a performance decay is reversible or not. **Figure S3** shows the results. As seen

here, for the cells with molecular weights of 25 K and 30 K, J_{SC} increases slightly after thermal annealing, indicating the partial recovery of J_{SC} decay. However, no noticeable V_{OC} and FF enhancement is found for all these cells after thermal annealing, indicating the V_{OC} and FF decay of these cells is not fully thermally reversible.

3. Morphology and optical properties of the blend films

It was reported that burn-in V_{OC} loss in polymer solar cells is highly dependent on the crystallinity of polymers, where amorphous polymer blend usually leads to fast V_{OC} decay.[17] Crystallinity of the P3HT:$PC_{61}BM$ blends were exmined in this work using UV-vis absorption, XRD and TEM. **Figure S4a**, **4b** and **Figure S5** in supporting information show the UV-Vis absorption spectra, XRD patterns and TEM images of P3HT:$PC_{61}BM$ with different P3HTs, respectively. As seen from **Figure S4a**, all these films showed broad absorption bands over 300-650 nm, where 0-0 and 0-1 transition absorptions (600 and 570 nm, respectively) can be clearly distinguished, which is ascribed to the intermolecular π-π stacking of P3HT backbones.[36] The XRD patterns of these films (**Figure S4b**) show show a diffraction peak at 2θ of 5.57°, corresponding to the lamellar structure of P3HT with an intermolecular distance of 1.57 Å,[37] indicating that all these P3HT blend films are highly crystalline. The TEM images (**Figure S5**) of the blend films also confirmed the formation of nanocrystals in these blend films, which is in good accordance with the XRD results. Both the XRD and TEM results demonstrate that all these P3HT:$PC_{61}BM$ films are highly crystalline, owing to the high regioregularity of the P3HTs (**Table 1**).

To check the changes of the morphology of these films during aiging, UV-Vis absorption and external quantum efficiency (EQE) spectra of these cells were measured. **Figure S6** and **S7** in supporting information show the results. As seen from **Figure S6**, the absorption of crystalline P3HT domains (over 500-650 nm)[36] decreases slightly with less pronounced 0-0 vibration bands, suggesting the slight decrease of the crystallinity of P3HT domain during aging, whereas the EQE spectra confirm a similar conclusion (**Figure S7**). However, there is no direct evidence that P3HT-20K based cells showed more significant UV-Vis and EQE changes after aging. In other words, there is no direct correlation between the morphology change of the blend film to the fast degration of P3HT-20K based cell.

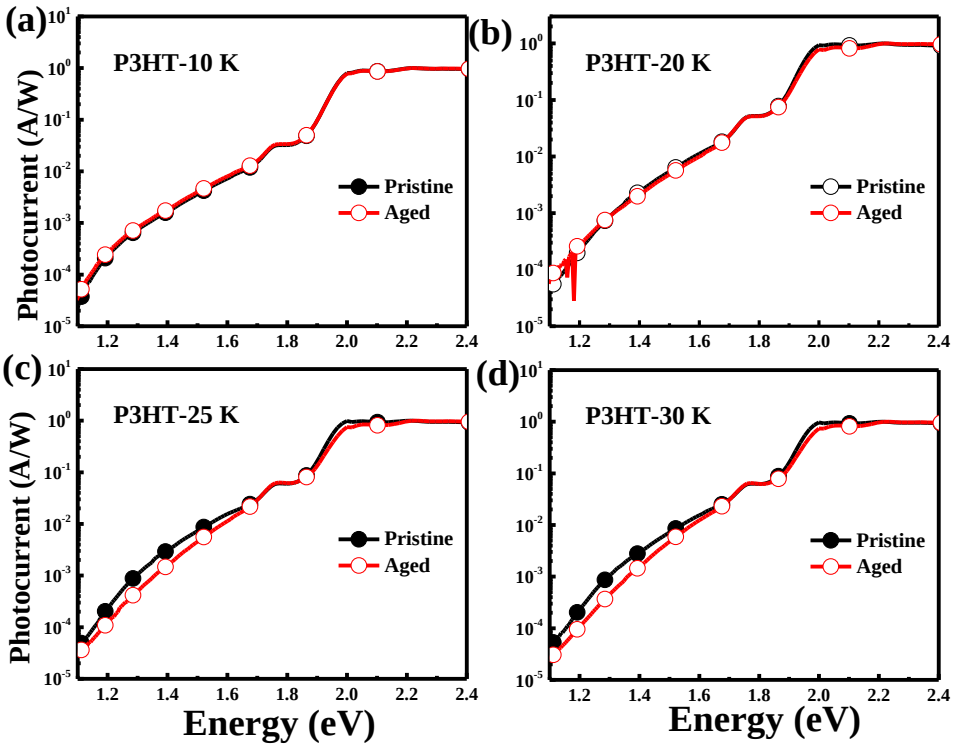

Figure 3. Fourier transform photocurrent spectroscopy of the pristine and aged P3HT:$PC_{61}BM$ cells

Janssen *et al.* reported that the charge transfer state (CT) of photoactive layer shows a significant influence on the V_{OC} of polymer solar cells.[38] To check whether the CT state of photoactive layer changes after aging, Fourier transform photocurrent spectroscopy (FTPS) of these cells were measured. **Figure 3** depicts the results, and the CT state was simulated according to the Marcus theory (see **Figure S8** in supporting information).[39] Results indicate that there is no significant changes of the charge transfer state for all these cells before and after aging. Together with the irreversibility of these cells during aging (*vide supra,* **Figure S3**), we concluded that the degradation of these cells should not be correlated to the changes of the crystallinity of P3HT domain.

Surface morphology of the blend films were then measured by atomic force microscope (AFM). **Figure 4** shows the topological AFM images of these films. As seen here, for all these films rough surfaces are measured with root mean surface roughnesses (Rms) of 16.9, 28.0, 15.2, and 12.0 nm, respectively. The rough surface could be due to the high crystallinity of these P3HTs. Interestingly, the film made of P3HT-20 K has the largest roughness, which will increase the interface connection between P3HT and thermally evaporated MoO_3 layer. Since open circuit voltage of polymer solar cells is

highly sensitive to the interfacial charge recombination, we therefore supeculate that interfacial degradation could be the main reason for the performance decay of this type of cells.

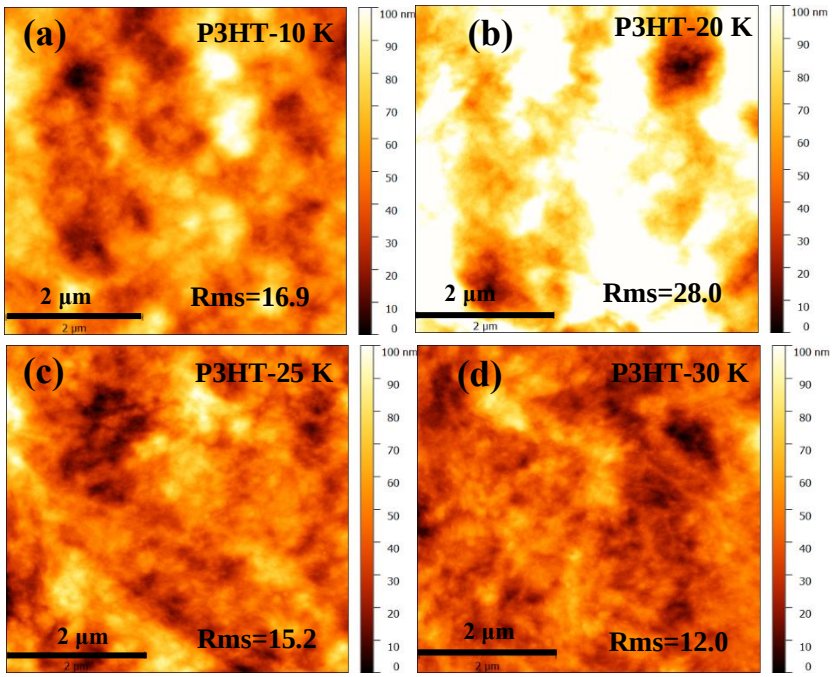

Figure 4. AFM topological image of P3HT:$PC_{61}BM$ films

4. Interfacial photoreduction of MoO_3 by P3HT

To understand the changes of the interface of the cell during aging, model interfaces with a structure of P3HT (15 nm)/MoO_3 (5 nm), $PC_{61}BM$ (15 nm)/MoO_3 (5 nm), and P3HT:$PC_{61}BM$ (15 nm)/MoO_3 (5 nm) based on P3HT-20 K were fabricated and aged under white light (using the same light source for the solar cell aging test). For comparison, reference MoO_3, P3HT and $PC_{61}BM$ films on ITO glass were also made and tested. The UV-Vis absorption spectra of these films illuminated at different times are shown in **Figure 5** and **Figure S9**. As seen from **Figure S9a-c**, no obvious absorption changes can be detected for MoO_3, $PC_{61}BM$, $PC_{61}BM/MoO_3$ films, suggesting that properties of these three films do not change under light illumination. In contrast, for P3HT:$PC_{61}BM/MoO_3$ and P3HT/MoO_3 films (**Figure 5a** and **5b**), absorption enhancement over 400-650 nm can be clearly seen. Note that both pure P3HT and P3HT:PCBM films on ITO glass show almost no absorption change under light illumination (**Figure 5c** and **Figure S9d**), and all these samples are placed onto a

cold plate with a temperature of 25 ºC, such an absorption enhancement can not be attributed to the increase of the crystallinity of P3HT as a result of the heating effect of light illumination. Note also that there is no obvious absorption changes for P3HT/MoO_3 film kept in the dark (**Figure S9e**). The enhancement of absorption for the P3HT:$PC_{61}BM$/MoO_3 and P3HT/MoO_3 indicates that there is intensive interaction between P3HT and MoO_3 under light illumination.

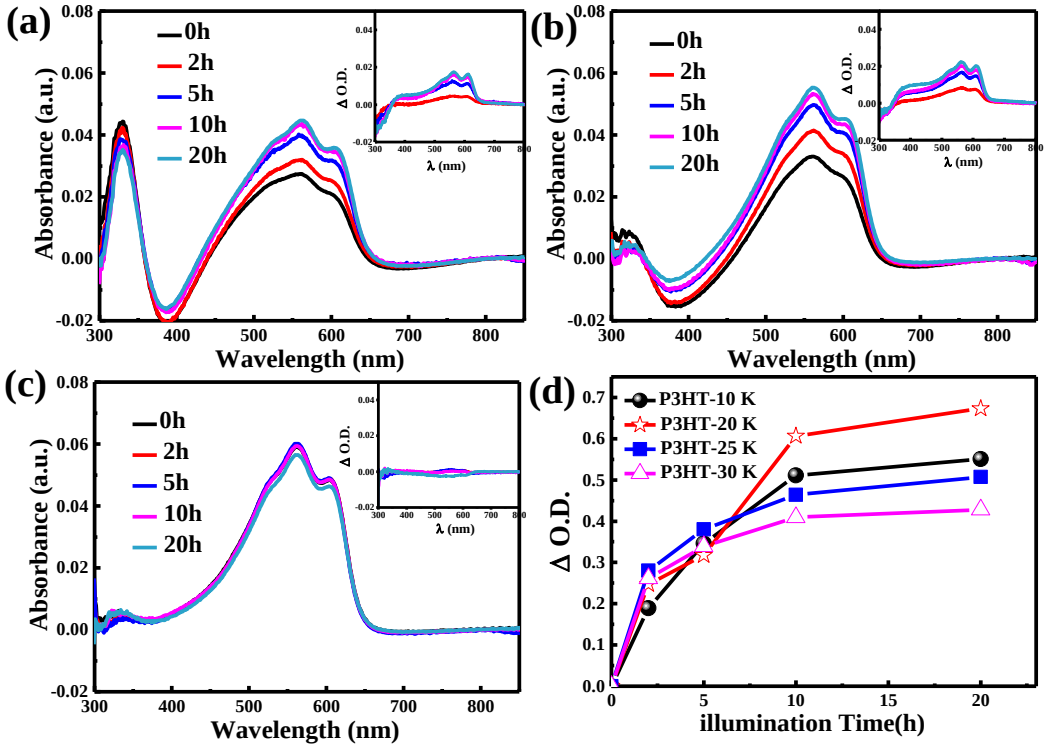

Figure 5. UV-Vis absorption spectra of P3HT -20 K:PCBM/MoO_3(a), P3HT-20 K/MoO_3(b) and P3HT(c) films illuminated with LED white light for different hours (at 25 ºC); The insertion is the optical density difference for the films after illuminated with light for different times; (d) absorbance changes at 560 nm for different P3HT illuminated under light for a certain time.

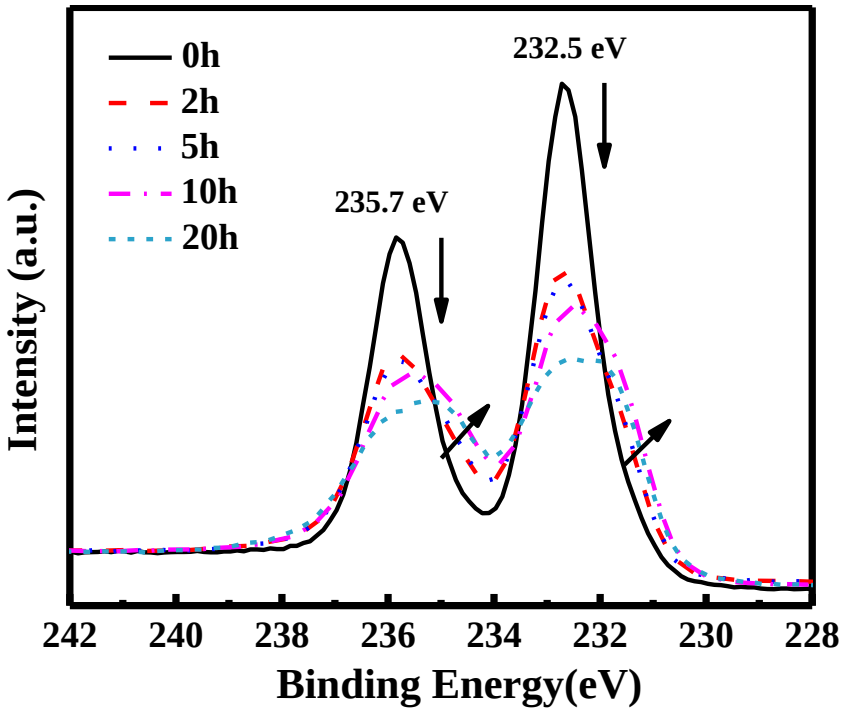

Figure 6. XPS spectra of Mo of P3HT/ MoO_3 films under light illumination for different times.

It was reported that the oxidization of P3HT would lead to the formation of quinoid structure of P3HT backbone, which will enhance the π-π interaction between P3HT chains and consequently increase the 0-0 transition absorption.[36, 40] Photon induced electron transfer from P3HT to MoO_3 is then proposed to be the main chemical reaction between these two components. To further confirm such a photochemical reaction between P3HT and MoO_3, the P3HT (20 K, 15 nm)/MoO_3 (5 nm) films illuminated with different times were checked with X-ray photoelectron spectroscopy (XPS). **Figure 6** shows the XPS of Mo 3d of the films with different illumination time. Forfresh P3HT/MoO_3 film, two typical peaks at 232.5 eV and 235.7 eV were measured, which can be attributed to the signals of Mo^{6+}.[41] With the increase of light illumination time, the XPS peaks turn to be broader and less intensive. By peak fitting (See **Figure S11** in Supporting Information), two sets of peaks with the value of 232.5/235.7 eV, and 231.4/234.6 eV can be deduced, which can be attributed to the signal of Mo^{6+} and Mo^{5+}, respectively. This result indicates that Mo^{6+} is partially reduced by P3HT under light illumination.

Figure S10 in supporting information shows the absorption spectra of P3HT:$PC_{61}BM$ and P3HT films with different molecular weight under light illumination. Both the films

with or/without MoO_3 layer were measured. Similar to P3HT-20K based films, all films without MoO_3 layer do not show obvious absorption changes under light illumination. In contrast, films with MoO_3 layer show characteristic absorption enhancement over 400-650 nm, confirming the generality of such photon chemical interaction between P3HT and MoO_3. The absorption enhancement over the illumination time for different P3HT is plotted in **Figure 5d**. As seen here, P3HT-20 K shows a much faster absorption enhancement than other P3HTs, which is in good accordance with the device stability of the P3HT based cells (**Figure 2**), further confirming that interfacial photochemical reduction of MoO_3 by P3HT should be the main reason for the fast V_{OC} and FF decay of P3HT-20 K cells.

5. V_{OC} and FF recovery after renewing the MoO_3/Al electrode

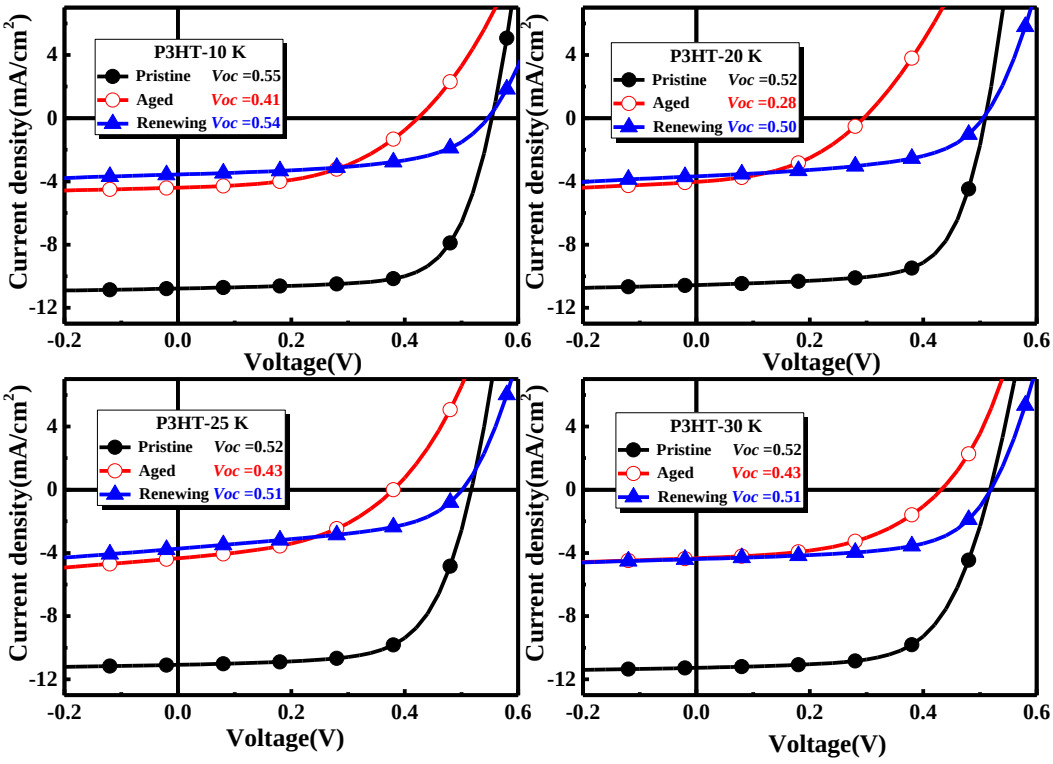

Figure 7. *J-V* curves of pristine cells, aged cells and the aged cells with renewed MoO_3/Al electrodes

To further confirm that interfacial degradation is the main reason causes the fast V_{OC} and FF decay of these cells, we renewed the MoO_3/Al electrode of the aged cells and tested the performance of the cells. By using dilute NaOH solution, we are able to remove the MoO_3/Al electrode of the cells without influencing photoactive layer.[16]

Figure 7 shows the *J-V* curves of pristine cells, aged cells, and the aged cells with renewed MoO_3/Al electrode, and the photovoltaic performance data are listed in **Table S1** in supporting information. In all cells with different P3HT, J_{SC} is not recovered after renewing the top electrode. However, both V_{OC} and FF increase with the renewed MoO_3/Al electrode. For example, the V_{OC} of aged P3HT-20 K cells is 0.28 V, which increases to 0.50 V after renewing the MoO_3/Al electrode, close to that of fresh cell (0.52 V). These results unambiguously confirm that interfacial degradation is the main reason for the V_{OC} and FF decay of cells. It is known that the P3HT-20K:$PC_{61}BM$ has a rougher surface than other P3HTs, which increases the interconnection between P3HT and MoO_3 and consequently enchances the interfacial photon chemical reaction. This results corresponding well to the fastest V_{OC} and FF decay of the P3HT-20K based cells. With that, an interfacial photochemical reaction between P3HT and MoO_3 is then proposed as shown in Figure 8, where the direct connection of P3HT with MoO3 leads to the formation of Mo5+ under light illumination, which increase interfacial charge recombination and consequently reduce the V_{OC} and FF of the cells. These results suggest that new interfacial materials that doesn't react with conjugated polymer is highly need to achieve highly stable polymer solar cells.

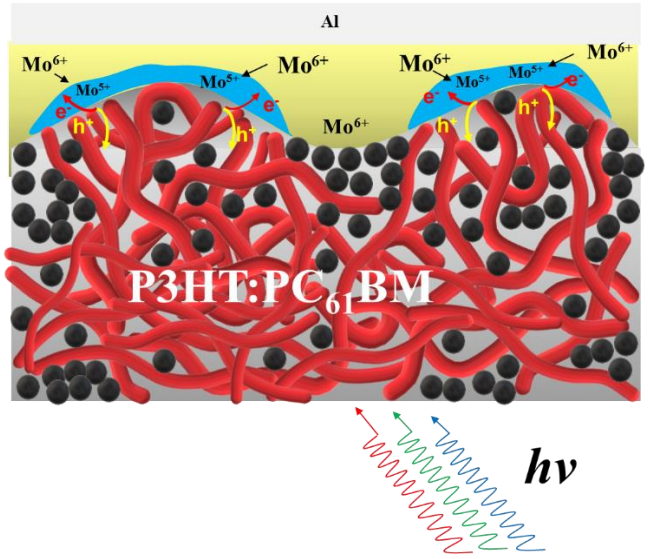

Fiugure 8. Interfacial photochemical reduction of MoO_3 by P3HT that causes fast V_{OC} and FF decay of the cell

Conclusion

In conclusion, the influence of the molecular weight of P3HT on performance and stability of P3HT:$PC_{61}BM$ cells was investigated. The V_{OC} and FF decays of the cell based on P3HT with a molecular weight of 20 K is much faster than those based on other P3HTs. The recovery of V_{OC} and FF was achieved for the aged cells after renewing the MoO_3/Al electrode, demonstrating that interfacial degradation at the photoactive layer/MoO_3 interface should be the main reason for the performance decay. Photochemical reduction of MoO_3 by P3HT was confirmed by the increased UV-vis absorption over 400-650 nm and the formation of Mo^{5+} as proved by the broadening and shifting of the XPS peaks from 232.5/235.7 eV to 231.4/234.6 eV, during light illumination. For the first time, it was clearly demonstrated that unexpected interfacial photochemical reaction at the anode could also lead to "burn-in" performance decay. Surface morphology analysis revealed the roughest surface of P3HT-20 K, which contributed to the fastest performance decay of P3HT-20K based cells.

Acknowledgment

The authors would like to acknowledge the financial support from the Ministry of Science and Technology of China (No. 2016YFA0200700), Chinese Academy of Science (No. YJKYYQ20180029, and CAS-ITRI 2019010), the National Natural Science Foundation of China (61904121), Youth Innovation Promotion Association, CAS (2019317). And the support of Suzhou Vacuum Interconnected Nanotechnology Workstation H005-2019 project. WWHW and SS are supported by the Australian Renewable Energy Agency through the Australian Centre for Advanced Photovoltaics as well as the ARC Centre of Excellence in Exciton Science (CE170100026).

Conflict of Interest

The authors declare no conflict of interest.

References:

1. Krebs, F. C.; Espinosa, N.; Hösel, M.; Søndergaard, R. R.; Jørgensen, M., 25th anniversary article: rise to power–OPV‐based solar parks. *Advanced Materials* **2014,** *26* (1), 29-39.
2. Hou, J.; Inganäs, O.; Friend, R. H.; Gao, F., Organic solar cells based on non-fullerene acceptors. *Nature Materials* **2018,** *17* (2), 119-128.
3. Lu, L.; Zheng, T.; Wu, Q.; Schneider, A. M.; Zhao, D.; Yu, L., Recent advances in bulk heterojunction polymer solar cells. *Chemical Reviews* **2015,** *115* (23), 12666-12731.
4. Yan, T.; Song, W.; Huang, J.; Peng, R.; Huang, L.; Ge, Z., 16.67% Rigid and 14.06% Flexible Organic Solar Cells Enabled by Ternary Heterojunction Strategy. *Advanced Materials* **2019,** *31* (39), 1902210.
5. Cui, Y.; Yao, H.; Zhang, J.; Zhang, T.; Wang, Y.; Hong, L.; Xian, K.; Xu, B.; Zhang, S.; Peng, J., Over 16% efficiency organic photovoltaic cells enabled by a chlorinated acceptor with increased open-circuit voltages. *Nature Communications* **2019,** *10* (1), 2515.
6. Lin, Y.; Adilbekova, B.; Firdaus, Y.; Yengel, E.; Faber, H.; Sajjad, M.; Zheng, X.; Yarali, E.; Seitkhan, A.; Bakr, O. M., 17% Efficient Organic Solar Cells Based on Liquid Exfoliated WS2 as a Replacement for PEDOT: PSS. *Advanced Materials* **2019** *31*(46), 1902965..
7. Meng, L.; Zhang, Y.; Wan, X.; Li, C.; Zhang, X.; Wang, Y.; Ke, X.; Xiao, Z.; Ding, L.; Xia, R., Organic and solution-processed tandem solar cells with 17.3% efficiency. *Science* **2018,** *361* (6407), 1094-1098.
8. Du, X.; Heumueller, T.; Gruber, W.; Classen, A.; Unruh, T.; Li, N.; Brabec, C. J., Efficient polymer solar cells based on non-fullerene acceptors with potential device lifetime approaching 10 years. *Joule* **2019,** *3* (1), 215-226.
9. Mateker, W. R.; Sachs-Quintana, I.; Burkhard, G. F.; Cheacharoen, R.; McGehee, M. D., Minimal long-term intrinsic degradation observed in a polymer solar cell illuminated in an oxygen-free environment. *Chemistry of Materials* **2015,** *27* (2), 404-407.
10. Martynov, I.; Akkuratov, A. V.; Luchkin, S.; Tsarev, S.; Babenko, S. D.; Petrov, V. G.; Stevenson, K. J.; Troshin, P. A., Impressive radiation stability of organic solar cells based on fullerene derivatives and carbazole-containing conjugated polymers. *ACS Applied Materials & Interfaces* **2019**.
11. Gevorgyan, S. A.; Espinosa, N.; Ciammaruchi, L.; Roth, B.; Livi, F.; Tsopanidis, S.; Züfle, S.; Queirós, S.; Gregori, A.; Benatto, G. A. d. R., Baselines for lifetime of organic solar cells. *Advanced Energy Materials* **2016,** *6* (22), 1600910.
12. Peters, C. H.; Sachs‐Quintana, I.; Mateker, W. R.; Heumueller, T.; Rivnay, J.; Noriega, R.; Beiley, Z. M.; Hoke, E. T.; Salleo, A.; McGehee, M. D., The mechanism of burn‐in loss in a high efficiency polymer solar cell. *Advanced Materials* **2012,** *24* (5), 663-668.
13. Reese, M. O.; Nardes, A. M.; Rupert, B. L.; Larsen, R. E.; Olson, D. C.; Lloyd, M. T.; Shaheen, S. E.; Ginley, D. S.; Rumbles, G.; Kopidakis, N., Photoinduced degradation of polymer and polymer–fullerene active layers: experiment and theory. *Advanced Functional Materials* **2010,** *20* (20), 3476-3483.
14. Distler, A.; Sauermann, T.; Egelhaaf, H. J.; Rodman, S.; Waller, D.; Cheon, K. S.; Lee, M.; Guldi, D. M., The effect of PCBM dimerization on the performance of bulk heterojunction solar cells. *Advanced Energy Materials* **2014,** *4* (1), 1300693.
15. Heumueller, T.; Mateker, W. R.; Distler, A.; Fritze, U. F.; Cheacharoen, R.; Nguyen, W. H.; Biele, M.; Salvador, M.; von Delius, M.; Egelhaaf, H.-J., Morphological and electrical control of fullerene dimerization determines organic photovoltaic stability. *Energ Environ Sci* **2016,** *9* (1), 247-256.
16. Yan, L.; Yi, J.; Chen, Q.; Dou, J.; Yang, Y.; Liu, X.; Chen, L.; Ma, C.-Q., External load-dependent degradation of P3HT: PC 61 BM solar cells: behavior, mechanism, and method of suppression. *Journal of Materials*

Chemistry A **2017,** *5* (20), 10010-10020.

17. Heumueller, T.; Mateker, W. R.; Sachs-Quintana, I.; Vandewal, K.; Bartelt, J. A.; Burke, T. M.; Ameri, T.; Brabec, C. J.; McGehee, M. D., Reducing burn-in voltage loss in polymer solar cells by increasing the polymer crystallinity. *Energy & Environmental Science* **2014,** *7* (9), 2974-2980.
18. Heumueller, T.; Burke, T. M.; Mateker, W. R.; Sachs‐Quintana, I. T.; Vandewal, K.; Brabec, C. J.; McGehee, M. D., Disorder‐Induced Open‐Circuit Voltage Losses in Organic Solar Cells During Photoinduced Burn‐In. *Advanced Energy Materials* **2015,** *5* (14), 1500111.
19. Li, N.; Perea, J. D.; Kassar, T.; Richter, M.; Heumueller, T.; Matt, G. J.; Hou, Y.; Güldal, N. S.; Chen, H.; Chen, S., Abnormal strong burn-in degradation of highly efficient polymer solar cells caused by spinodal donor-acceptor demixing. *Nature Communications* **2017,** *8*, 14541.
20. Sachs‐Quintana, I.; Heumüller, T.; Mateker, W. R.; Orozco, D. E.; Cheacharoen, R.; Sweetnam, S.; Brabec, C. J.; McGehee, M. D., Electron Barrier Formation at the Organic‐Back Contact Interface is the First Step in Thermal Degradation of Polymer Solar Cells. *Advanced Functional Materials* **2014,** *24* (25), 3978-3985.
21. Jiang, Y.; Sun, L.; Jiang, F.; Xie, C.; Hu, L.; Dong, X.; Qin, F.; Liu, T.; Hu, L.; Jiang, X., Photocatalytic effect of ZnO on the stability of nonfullerene acceptors and its mitigation by SnO 2 for nonfullerene organic solar cells. *Materials Horizons* **2019**, *6* (7), 1438--1443..
22. Park, S.; Son, H. J., Intrinsic photo-degradation and mechanism of polymer solar cells: the crucial role of non-fullerene acceptors. *Journal of Materials Chemistry A* **2019,** *7* (45), 25830–25837.
23. Woo, C. H.; Thompson, B. C.; Kim, B. J.; Toney, M. F.; Fréchet, J. M., The influence of poly (3-hexylthiophene) regioregularity on fullerene-composite solar cell performance. *Journal of the American Chemical Society* **2008,** *130* (48), 16324-16329.
24. Chandrasekaran, N.; Liu, A. C.; Kumar, A.; McNeill, C. R.; Kabra, D., Effect of regioregularity on recombination dynamics in inverted bulk heterojunction organic solar cells. *Journal of Physics D: Applied Physics* **2017,** *51* (1), 015501.
25. Schilinsky, P.; Asawapirom, U.; Scherf, U.; Biele, M.; Brabec, C. J., Influence of the molecular weight of poly (3-hexylthiophene) on the performance of bulk heterojunction solar cells. *Chemistry of Materials* **2005,** *17* (8), 2175-2180.
26. Osaka, I.; Saito, M.; Mori, H.; Koganezawa, T.; Takimiya, K., Drastic change of molecular orientation in a thiazolothiazole copolymer by molecular‐weight control and blending with PC61BM leads to high efficiencies in solar cells. *Advanced Materials* **2012,** *24* (3), 425-430.
27. Subbiah, J.; Purushothaman, B.; Chen, M.; Qin, T.; Gao, M.; Vak, D.; Scholes, F. H.; Chen, X.; Watkins, S. E.; Wilson, G. J., Organic solar cells using a high‐molecular‐weight benzodithiophene–benzothiadiazole copolymer with an efficiency of 9.4%. *Advanced Materials* **2015,** *27* (4), 702-705.
28. Li, W.; Yang, L.; Tumbleston, J. R.; Yan, L.; Ade, H.; You, W., Controlling Molecular Weight of a High Efficiency Donor‐Acceptor Conjugated Polymer and Understanding Its Significant Impact on Photovoltaic Properties. *Advanced Materials* **2014,** *26* (26), 4456-4462.
29. Hiorns, R. C.; De Bettignies, R.; Leroy, J.; Bailly, S.; Firon, M.; Sentein, C.; Khoukh, A.; Preud'homme, H.; Dagron‐Lartigau, C., High molecular weights, polydispersities, and annealing temperatures in the optimization of bulk‐heterojunction photovoltaic cells based on poly (3‐hexylthiophene) or poly (3‐butylthiophene). *Advanced Functional Materials* **2006,** *16* (17), 2263-2273.
30. Loewe, R. S.; Khersonsky, S. M.; McCullough, R. D., A simple method to prepare head‐to‐tail coupled, regioregular poly (3‐alkylthiophenes) using Grignard metathesis. *Advanced Materials* **1999,** *11* (3), 250-253.
31. Beek, W. J.; Wienk, M. M.; Kemerink, M.; Yang, X.; Janssen, R. A., Hybrid zinc oxide conjugated polymer

bulk heterojunction solar cells. *The Journal of Physical Chemistry B* **2005,** *109* (19), 9505-9516.

32. Dang, M. T.; Hirsch, L.; Wantz, G., P3HT: PCBM, best seller in polymer photovoltaic research. *Advanced Materials* **2011,** *23* (31), 3597-3602.
33. Li, G.; Shrotriya, V.; Huang, J.; Yao, Y.; Moriarty, T.; Emery, K.; Yang, Y., High-efficiency solution processable polymer photovoltaic cells by self-organization of polymer blends. *World Scientific*: **2011**; 80-84.
34. Liu, F.; Chen, D.; Wang, C.; Luo, K.; Gu, W.; Briseno, A. L.; Hsu, J. W.; Russell, T. P., Molecular weight dependence of the morphology in P3HT: PCBM solar cells. *ACS Mpplied Materials & Interfaces* **2014,** *6* (22), 19876-19887.
35. Yan, L.; Wang, Y.; Wei, J.; Ji, G.; Gu, H.; Li, Z.; Zhang, J.; Luo, Q.; Wang, Z.; Liu, X., Simultaneous performance and stability improvement of polymer: fullerene solar cells by doping with piperazine. *Journal of Materials Chemistry A* **2019,** *7* (12), 7099-7108.
36. Ehrenreich, P.; Birkhold, S. T.; Zimmermann, E.; Hu, H.; Kim, K.-D.; Weickert, J.; Pfadler, T.; Schmidt-Mende, L., H-aggregate analysis of P3HT thin films-Capability and limitation of photoluminescence and UV/Vis spectroscopy. *Scientific Reports* **2016,** *6*, 32434.
37. Noguchi, Y.; Saeki, A.; Fujiwara, T.; Yamanaka, S.; Kumano, M.; Sakurai, T.; Matsuyama, N.; Nakano, M.; Hirao, N.; Ohishi, Y., Pressure modulation of backbone conformation and intermolecular distance of conjugated polymers toward understanding the dynamism of π-figuration of their conjugated system. *The Journal of Physical Chemistry B* **2015,** *119* (24), 7219-7230.
38. Veldman, D.; Meskers, S. C.; Janssen, R. A., The energy of charge‐transfer states in electron donor–acceptor blends: insight into the energy losses in organic solar cells. *Advanced Functional Materials* **2009,** *19* (12), 1939-1948.
39. Vandewal, K.; Tvingstedt, K.; Gadisa, A.; Inganäs, O.; Manca, J. V., Relating the open-circuit voltage to interface molecular properties of donor: acceptor bulk heterojunction solar cells. *Physical Review B* **2010,** *81* (12), 125204.
40. Nia, N. Y.; Lamanna, E.; Zendehdel, M.; Palma, A. L.; Zurlo, F.; Castriotta, L. A.; Di Carlo, A., Doping Strategy for Efficient and Stable Triple Cation Hybrid Perovskite Solar Cells and Module Based on Poly (3‐hexylthiophene) Hole Transport Layer. *Small* **2019**, *15* (49), 1904399.
41. He, T.; Yao, J., Photochromism of molybdenum oxide. *Journal of Photochemistry and Photobiology C: Photochemistry Reviews* **2003,** *4* (2), 125-143.